bridge between two strongly bonded ruthenium atoms.[11,13]

The structure was determined by a single-crystal X-ray diffraction study.[14] An ORTEP II plot is illustrated in Figure 1, which also provides bond length data (inset) for the metal framework. The five ruthenium atoms form a square-based pyramid with Ru(1), Ru(2), Ru(4), and Ru(5) defining the base and Ru(3), the apex. Apical Ru(3) lies 2.086 Å above the best plane[15] defined by the four basal metal atoms and is slightly displaced away from the basal edge [Ru(4)–Ru(5)] bridged by the phosphido group. The base of the pyramid is slightly but significantly distorted toward a rectangle with the shorter Ru–Ru bond [Ru(4)–Ru(5) = 2.696 (1) Å] bridged by a phosphido group occupying equatorial sites. The remaining seven Ru–Ru distances (average, 2.855 Å) are normal, as compared to bond lengths in other ruthenium clusters,[16] with no single bond length deviating by more than 0.04 Å from the mean. The lack of structural data for any other square-pyramidal $Ru_5$ cluster precludes a more detailed analysis. The acetylide which bridges the Ru(4)–Ru(5) edge in symmetrical fashion is simultaneously $\eta$ bonded to the remaining two basal atoms Ru(1) and Ru(2). The Ru(4)–C(14) [2.114 (8) Å] and Ru(5)–C(14) [2.095 (8) Å] distances are significantly shorter than the corresponding Ru–C (acetylide) distances [Ru(2)–C(19) 2.22(1) and Ru(3)–C(19) 2.185(9) Å] in $Ru_3(CO)_6$ ($\mu_2$-C≡Bu-$t$)$_2$($PPh_2$)$_2$($Ph_2PC_2$Bu-$t$)[17] where, however, the symmetrically bridging acetylide is not involved in $\eta$ bonding with other metal atoms. Comparison of ruthenium–carbon (acetylide) bond lengths in $Ru_5(CO)_{13}(\mu_4$-$C_2Ph)(PPh_2)$ [Ru(1)–C(14) 2.190 (8), Ru(1)–C(15) 2.216 (8), Ru(2)–C(14) 2.234(8), Ru(2)–C(15) 2.163(9) Å] with corresponding values in $Ru_3(CO)_9(\mu_3$-$C_2Pr$-$i)(PPh_2)$ [average Ru–C (acetylide) 2.321 Å] and $Ru_2(CO)_6$-($\mu_2$-$C_2$Bu-$t$)($PPh_2$)[11] [average Ru–C (acetylide) 2.350 Å] indicates a significant increase in the strength of metal–acetylide bonding as the number of interacting metal atoms increases. As a result of the strong $\eta$ interactions with Ru(1) and Ru(2), the carbon–carbon triple bond is lengthened to 1.342 (11) Å. This distance which is characteristic of uncoordinated alkene double bonds is the greatest we have yet observed for $\sigma$-$\eta$-acetylide complexes of group 8 metals.

Remarkably, the stereochemistry of the acetylenic carbon atom C(14) is planar[18] in contrast to the marked cis or trans bending at both carbon atoms which usually accompanies $\mu_2$- or $\mu_3$-alkyne or acetylide bonding. Figure 1 also illustrates that C(14) occupies a capping site on the Ru(1)–Ru(2)–Ru(4)–Ru(5) face, with the five ruthenium atoms and C(14) defining a distorted octahedron. This stereochemistry is reminiscent of the cluster carbide $Fe_5(CO)_{15}C$,[7] although in the present case the capping atom remains part of an acetylide. Athough a stereochemical similarity between $Fe_5(CO)_{13}C$ and $Ru_5(CO)_{13}$(C≡CPh)($PPh_2$) is evident, further speculation on a possible conversion of the latter to a cluster carbide and on the chemical behavior of the multisite-bound acetylide must await the results of experiments currently in progress.

Finally, in view of current interest in $^{31}P$ ($PPh_2$) chemical shift correlations with M–M bond lengths, we note that the very low field $^{31}P$ chemical shift of the $PPh_2$ group in $Ru_5(CO)_{13}$(C≡CPh)($PPh_2$) is consistent with the presence of a very strong Ru–Ru bond [Ru(4)–Ru(5) = 2.696 (1) Å] and short Ru–P bond lengths (average 2.286 Å) rather than an unusually small Ru(4)–P–Ru(5) angle.[19]

**Acknowledgment.** We are grateful to NSERC and Imperial Oil for financial support of this work.

**Supplementary Material Available:** Fractional atomic coordinates (Table S1), hydrogen atom coordinates and isotropic thermal parameters (Table S2), and anisotropic thermal parameters (Table S3) for $Ru_5(CO)_{13}(C_2Ph)(PPh_2)$ (3 pages). Ordering information is given on any current masthead page.

(14) Dark blue crystals of $Ru_5(CO)_{13}(C_2Ph)(PPh_2)$ are monoclinic, space group $P2_1/n$ with $a$ = 9.966 (2), $b$ = 16.877 (2), $c$ = 21.707 (4) Å; $\beta$ = 100.51 (2)°; $Z$ = 4; $\rho_m$ = 2.14, $\rho_c$ = 2.139 g cm$^{-3}$; $\mu_{MoK\alpha}$ = 21.15 cm$^{-1}$; $F(000)$ = 2208. The structure was solved and refined by using 3335 observed [$I \geq 3\sigma(I)$], independent reflections measured on a Syntex $P2_1$ automatic diffractometer using Mo K$\alpha$ radiation out to $2\theta \leq 45°$. With all nonhydrogen atoms having anisotropic thermal parameters and hydrogen atoms isotropic coefficients, the structure was refined by full-matrix least-squares methods to $R$ and $R_w$ values of 0.033 and 0.039, respectively.

(15) The atoms Ru(1), Ru(2), Ru(4), and Ru(5) deviated by less than ±0.02 Å from the mean plane through these atoms.

(16) Churchill, M. R.; Hollander, F. J.; Hutchinson, J. P. *Inorg. Chem.* **1977**, *16*, 2655–2659 and references therein.

(17) Carty, A. J.; Taylor, N. J.; Smith, W. F. *J. Chem. Soc., Chem. Commun.* **1979**, 750–751.

(18) The atom C(14) deviates by only 0.060 Å from a least-squares plane containing Ru(4), Ru(5), and C(15).

(19) The Ru(4)–P–Ru(5) angle of 72.30 (0)° does not differ markedly from the Ru–P–Ru angle [72.0 (0)° in $Ru_2(CO)_6$(C≡CBu-$t$)($PPh_2$) [$\delta$ ($^{31}P$) +123.9] but the Ru–Ru bond length, 2.752 (1) Å, and Ru–P distances (average, 2.339 Å) in the latter are significantly longer.

## Large, Inverse Solvent Isotope Effects: A Simple Test for the E1cB Mechanism[1]

James R. Keeffe*[†] and William P. Jencks

*Graduate Department of Biochemistry, Brandeis University Waltham, Massachusetts 02254*

*Received January 26, 1981*

We wish to report a large, inverse solvent deuterium isotope effect on the initial rates of base-induced *p*-nitrostyrene formation from [$\beta$-(*p*-nitrophenyl)ethyl]ammonium ions in aqueous acetohydroxamate buffers (eq 1). For compounds **1a** and **1b**, the

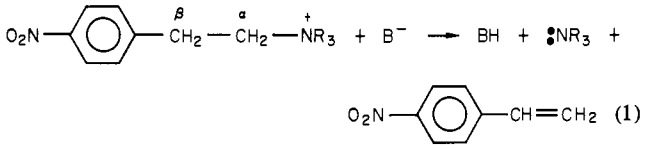

(1)

**1a**, :$NR_3$ = trimethylamine (p$K_a$ = 9.85)
**b**, :$NR_3$ = quinuclidine (p$K_a$ = 11.45)
**c**, :$NR_3$ = 4-methyl-1,4-diazabicyclo[2.2.2]octanium (p$K_a$ = 3.01)[2]

magnitude of the inverse effect can be increased by increasing the buffer concentration (at constant buffer ratio). This variation is quantitatively accounted for by application of the steady-state approximation to the ElcB mechanism (eq 2) and serves as a

$$\text{>C—H} \underset{k_{-1}[BH]}{\overset{k_1[B^-]}{\rightleftharpoons}} \text{>C}^- \xrightarrow{k_2} \text{products} \qquad (2)$$

sensitive test for that mechanism *whenever the proton-transfer step is not entirely rate controlling.*

In the figure are shown plots of experimental first-order rate constants for reaction of compound **1b** in $H_2O$ and $D_2O$, both against acetohydroxamate concentration. Three features are of interest: (1) The plots are curved. For the reaction in $H_2O$, buffer saturation is observed indicating a complete change of rate control from step 1 (proton transfer) to step 2 (leaving group departure). The buffer curvature for both solvents is quantitatively described by the steady-state analysis of the E1cB mechanism (see below) from which the lines through the experimental points were calculated. Similar, but less marked, curvature has been observed previously with increasing concentrations of substituted-quinuclidine buffers in $H_2O$.[2] (2) The observed rate constants are larger in $D_2O$ than in $H_2O$. (3) The inverse solvent isotope effect

[†]Department of Chemistry, San Francisco State University, San Francisco, CA 94132.

(1) A brief account of this work was presented at the Second Chemical Congress of the North American Continent, Las Vegas, NV, Aug 1980, ORGN 81. This is Publication 1352 from the Graduate Department of Biochemistry, Brandeis University, Waltham, MA 02254. This research was supported in part by grants from the National Science Foundation (PCM-7708369) and the National Institutes of Health (GM 20888).

0002-7863/81/1503-2457$01.25/0 

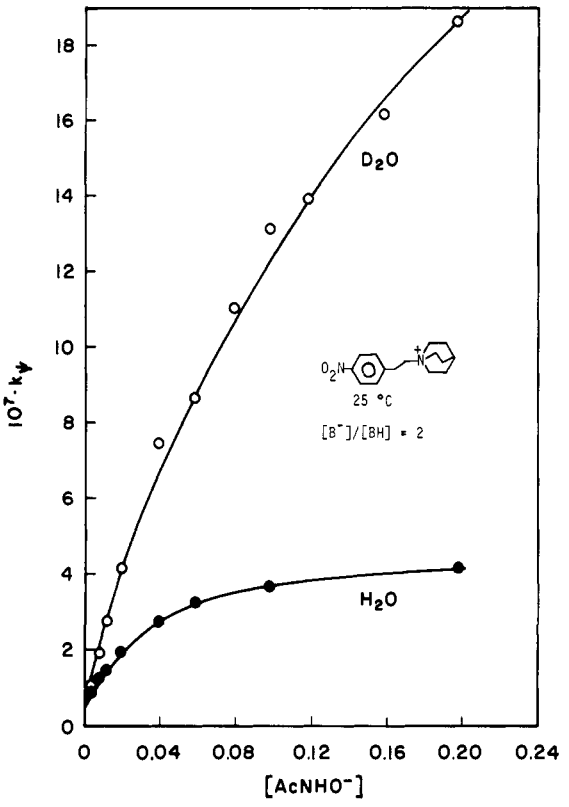


**Figure 1.** Plots of $k_{obsd}$ ($s^{-1}$) vs. [AcNLO⁻] for initial rates of *p*-nitrostyrene formation from **1b** in $H_2O$ and $D_2O$; $T$ = 25 °C, $\mu$ = 1.00 M (KCl). From that data we may calculate, among other quantities, $({}_Dk_1^H/{}_Hk_1^H)$ = 1.18 for acetohydroxamate catalysis. A value of 1.55 for hydroxide catalysis has been previously measured.[2] Primary isotope effects include $(k_{H_2O}/k_{D_2O})$ = 5.2 and $(k_{BH}/k_{BD})$ = 6.6 for protonation of the zwitterion by water and acetohydroxamic acid, respectively. The primary substrate isotope effect, $(k_1^H/k_1^D)$, is 8.5 with B⁻ = hydroxide.[2] The isotope effects for **1a** are very similar.

Scheme I

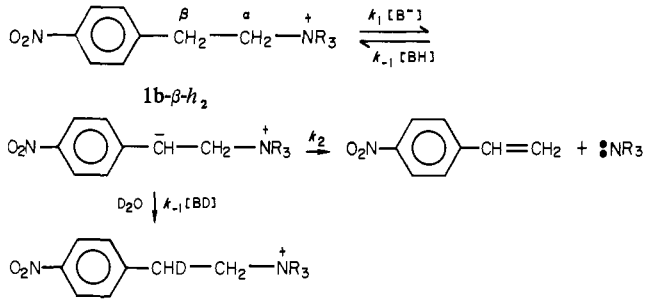


$({}_Dk_{obsd}/{}_Hk_{obsd})$, increases with [buffer]. An effect as large as 7.7 was measured at very early reaction times by using a buffer ratio [AcNLO⁻]/[AcNLOL] = 0.29 M/0.58 M. This is the largest published inverse solvent isotope effect of which we are aware. More O'Ferrall and Slae have described similar experimental results for the elimination of water or methanol from 9-fluorenylmethanol and 9-(methoxy)methylfluorene, for which an E1cB mechanism was assigned from other criteria.[3] In a separate experiment we observed isotopic hydrogen exchange at C-$\beta$ of **1b**, concurrent with elimination.

Qualitatively the inverse solvent isotope effects can be rationalized by means of Scheme I. At early times, *prior to significant exchange at C-$\beta$*, the substrate is essentially **1b**-$\beta$-$h_2$ regardless of the isotopic identity of the solvent. In $H_2O$ product formation is retarded by the reversal of step 1, i.e., $k_{-1}$[BH] competes with $k_2$. In $D_2O$, owing to a primary hydrogen isotope effect on reprotonation, $k_{-1}$[BD] does not compete so effectively with $k_2$, and the rate of product formation is not decreased as much as in $H_2O$ (we assume no significant isotope effect on $k_2$). As [buffer] is raised the partitioning of the intermediate will become dominated by $k_{-1}$[BH] in $H_2O$ at a point where $k_{-1}$[BD] in $D_2O$ does not yet dominate. That is, step 2 will become rate controlling in $H_2O$ at a buffer concentration where step 1 is still partly rate controlling in $D_2O$ and where ${}_Dk_{obsd}$ (but not ${}_Hk_{obsd}$) is increasing with added buffer.

The buffer curvature and the variable inverse solvent isotope effects establish the reaction path as a true E1cB mechanism. The initial rate via the E2 mechanism would not show such an inverse solvent isotope effect or buffer curvature, even if carbanion formation and isotopic exchange occurred concurrently.[4] A freely solvated intermediate is required. An E1cB (ion pair) mechanism also would not show such behavior, unless there is rapid exchange of deuterium into the $BH^+$–carbanion complex.

Quantitatively the observed rates are described by the steady-state rate law for the E1cB mechanism (eq 3). The inverse

$$ {}_Lk_{obsd}\ (s^{-1}) = \frac{k_1[B^-]k_2}{k_{-1}[BL] + k_2} = \frac{(k_{OL}[OL^-] + k_B[AcNLO^-])k_2}{(k_{L_2O} + k_{BL}[AcNLOL]) + k_2} \quad (3) $$

solvent isotope effects (assuming ${}_Hk_2 \simeq {}_Dk_2$) are given by eq 4.

$$ ({}_Dk_{obsd}/{}_Hk_{obsd}) = ({}_Dk_1^H/{}_Hk_1^H)\left(\frac{{}_Hk_{-1}^H[BH] + k_2}{{}_Dk_{-1}^D[BD] + k_2}\right) \quad (4) $$

The superscripts refer to the transferred isotope while the subscripts denote the isotopic identity of the solvent. Despite the fact that $k_1$ contains two terms, $({}_Dk_1^H/{}_Hk_1^H)$ depends only slightly on [buffer].[5] Thus the magnitude of $({}_Dk_{obsd}/{}_Hk_{obsd})$ depends principally on $({}_Hk_{-1}^H/{}_Dk_{-1}^D)$ and the extent to which ${}_Hk_{-1}^H$[BH] and ${}_Dk_{-1}^D$[BD] dominate the sums, ${}_Lk_{-1}^L$[BL] + $k_2$, in eq 4. The observed inverse effect increases from a minimum value at very low [buffer] ($k_2 \gg k_{-1}$ [BL]; step 1 rate controlling) to a maximum at high [buffer], at which step 2 becomes rate controlling and the ratio is given by eq 5. Equation 5 would apply even at

$$ ({}_Dk_{obsd}/{}_Hk_{obsd}) = ({}_Dk_\infty/{}_Hk_\infty) \simeq ({}_Dk_1^H/{}_Hk_1^H)({}_Hk_{-1}^H/{}_Dk_{-1}^D) \quad (5) $$

low [buffer] were reprotonation by solvent alone faster than step 2.

Finally we note that the E1cB mechanism contains the implication that better leaving groups bias the reaction toward the E1cB (irreversible) variant. Using eq 3 we calculate the partitioning ratio $k_{BH}/k_2$ = 85 $M^{-1}$ for **1b**, 1.8 $M^{-1}$ for **1a**, and <0.01 $M^{-1}$ for **1c** for which, in fact, neither buffer curvature nor variable, inverse solvent isotope effects were observed.[6] The results for **1a** are instructive. Buffer curvature in $H_2O$ could be seen and isotopic hydrogen exchange at C-$\beta$ was demonstrated. Neither result was dramatic owing to the relatively unfavorable partitioning ratio. Nevertheless the variable, inverse solvent isotope effect was easily detected and qualifies therefore as a sensitive signal for the E1cB mechanism.

Large inverse isotope effects can be observed for the initial rates of reactions involving proton abstraction from carbon when a second step is largely rate determining because the first step is

(2) Alunni, S.; Jencks, W. P. *J. Am. Chem. Soc.* **1980**, *102*, 2052–2060.

(3) More O'Ferrall and Slae (More O'Ferrall, R. A.; Slae, S. *J. Chem. Soc. B* **1970**, 260–268) used a combination of isotope effects to decide that the dehydration of 9-fluorenylmethanol in aqueous sodium hydroxide follows (principally) the E1cB (reversible) path. Although they do not discuss the point, their data appear to allow the analysis made in this communication. Thus $({}_Dk^H_{obsd}/{}_Hk^H_{obsd})$ = 14.3/1.81 (their Tables 2 and 5) = 7.9. A guess that $({}_Dk_1^H/{}_Hk_1^H)$, OL⁻, ~1.6 allows the estimate that $(k_{H_2O}/k_{D_2O})$ ~4.9, a primary isotope effect for protonation of a carbanion by water which is very similar to our results (see legend for Figure 1). Similar results were obtained for 9-(methoxy)methylfluorene in methanolic sodium methoxide (More O'Ferrall, R. A.; Warren, P. J. *Proc. R. Ir. Acad., Sect. B* **1977**, *77B*, 513–521).

(4) Breslow, R. S. *Tetrahedron Lett.* **1964**, 399–403.

(5) The inverse isotope effect on step 1 varies from 1.5 at very low [buffer] to 1.2 at high [buffer]; see legend for Figure 1.

(6) All compounds **1** and four other [$\beta$-(*p*-nitrophenyl)ethyl]ammonium ions fall on the same line of slope $\beta_{lg}$ = −0.17 in a plot of log $k_1$ against $pK_{R_3NH^+}$; this small slope is characteristic of a transition state involving only proton abstraction in the initial step of an E1cB mechanism.[2]

a pseudo-equilibrium[7] that incorporates a primary kinetic isotope effect; i.e., it is determined by the ratio of the rate constants for H removal in the forward direction and D addition in the reverse direction.[8] In contrast, the observed isotope effect will depend largely on the equilibrium isotope effect for the first step in reactions involving initial reversible protonation of carbon[9] or in the later stage of E1cB (reversible) elimination reactions, after complete exchange with the solvent has occurred.[3]

(7) Long, F. A.; Bakule, R. *J. Am. Chem. Soc.* **1963**, *85*, 2313–2323.

(8) Littler, J. S.; Quick, G. R.; Wozniak, D. *J. Chem. Soc., Perkin Trans. 2* **1980**, 657–661, have observed this behavior for the initial rate of cyclohexanone oxidation through the enol in acid solution, which gives inverse solvent isotope effects of 4.9–5.9 and is first order in the oxidant. The initial rate also shows a normal primary isotope effect with deuterated substrate under conditions in which the oxidation step is rate determining because the $k_1$ step involved H or D, whereas $k_{-1}$ always involves H. The same behavior has been observed for the isomerization of dihydroxyacetone phosphate catalyzed by triose phosphate isomerase, which exhibits a primary isotope effect because of this pseudo-equilibrium under conditions in which proton transfer is not rate determining (Leadlay, P. F.; Albery, W. J.; Knowles, J. R. *Biochemistry* **1976**, *15*, 5617–5620).

(9) The acid-catalyzed hydrolysis of a cyclic vinyl ether has been reported to undergo a leveling of the rate as the buffer concentration increases, with an inverse solvent deuterium isotope effect at high buffer concentration that represents such an equilibrium isotope effect (Cooper, J. D.; Vitullo, V. P.; Whalen, D. L. *J. Am. Chem. Soc.* **1971**, *93*, 6294–6296).

## Asymmetric Synthesis of α-Amino Acids Using Chiral Cobalt(III) Complexes

Masanobu Ajioka, Shigenobu Yano,* Kenichi Matsuda, and Sadao Yoshikawa*

*Department of Synthetic Chemistry, Faculty of Engineering The University of Tokyo, Hongo, Bunkyo-ku Tokyo 113, Japan*

*Received November 12, 1980*

We have developed a novel asymmetric synthesis of α-amino acids by using chiral cobalt(III) complexes containing 1,5*R*,7*R*,11-$Me_4$-2,3,2-tet[1] as a ligand.

Some studies have been reported on the asymmetric synthesis of α-amino acids[2,3] and asymmetric transformation of α-amino acids[4–6] in their chiral cobalt(III) complexes. In every case, however, amino acids were not isolated from the cobalt(III) complexes until they were subjected to a decomposition process which often accompanied racemization of the amino acids.

We recently discovered a new type of reaction to isolate amino acids with retention of the asymmetric carbon center from the cobalt(III) complexes under mild conditions while also preserving the complexes.

When Λ-β$_2$-[Co(*R* or *S*-Ala)(1,5*R*,7*R*,11-$Me_4$-2,3,2-tet)]$^{2+}$ was warmed in an 0.1 M $Na_2CO_3$ aqueous solution at 50 °C for 30 min, the starting red solution changed its color to violet. The reaction in a 0.1 M $Na_2CO_3$–$D_2O$ solution was followed by $^1$H NMR spectroscopy. The *C*-methyl signal of the coordinated alanine gradually decreased to zero. This color change corresponds also to the shift of absorption maximum in the visible spectrum from 513 to 530 nm. The reaction mixture was loaded on an SP-Sephadex (C-25) cation exchange resin. The colored fraction was adsorbed on the resin. The solution passed through the column was confirmed to contain free alanine by an amino acid analyzer. This free alanine was converted to 2,4-dinitrophenylalanine (DNP-alanine). The DNP-alanine was purified by silica gel thin-layer chromatography. The specific optical rotation of the authentic DNP-(*S*)-alanine was compared with that of the DNP-alanine prepared from pure (*R*)-alaninato or (*S*)-alaninato complex. The comparison indicated that the asymmetry of alanine was retained quantitatively (>99%) during the release.[11]

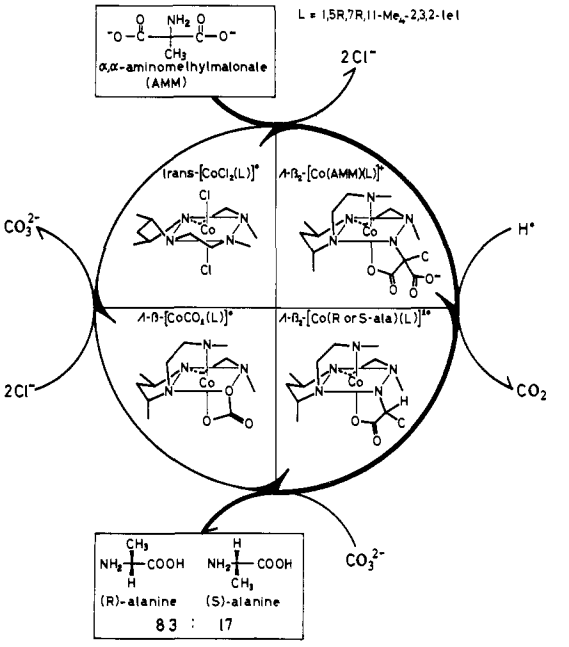


**Figure 1.**

The $^1$H NMR, electronic absorption (AB), and CD data for the complex eluted with a 0.05 N $NaClO_4$ solution agreed well with those for the carbonato complex represented as Λ-β-[$CoCO_3$(1,5*R*,7*R*,11-$Me_4$-2,3,2-tet)]$ClO_4$·$H_2O$.[7] This carbonato complex was easily converted to the starting trans-dichloro complex of 1,5*R*,7*R*,11-$Me_4$-2,3,2-tet. The new asymmetric synthesis of α-amino acids described above is depicted in Figure 1.

The first step of this cyclic system is the introduction of α-amino-α-methylmalonic acid (AMM) into the starting *trans*-dichloro complex. The *trans*-[$CoCl_2$(1,5*R*,7*R*,11-$Me_4$-2,3,2-tet)]$ClO_4$ (0.89 g) and ammonium α-amino-α-methylmalonate (0.33 g) were refluxed in 100 mL of methanol. The product was purified through an SP-Sephadex (C-25) cation exchange resin column and isolated as the perchlorate salt. On the basis of analytical and spectral data, the complex was assigned as Λ-β$_2$-[Co(AMM)(1,5*R*,7*R*,11-$Me_4$-2,3,2-tet)]$ClO_4$·2·5$H_2O$ and obtained stereospecifically.[8]

The second step is the decarboxylation of AMM on the complex. The AB, CD, and $^1$H NMR spectra of the product decarboxylated from Λ-β$_2$-[Co(AMM)(1,5*R*,7*R*,11-$Me_4$-2,3,2-tet)]$^+$ in 1 N hydrochloric acid at 70 °C were almost the same as those of Λ-β$_2$-[Co(*R*-Ala)(1,5*R*,11-$Me_4$-2,3,2-tet)]$^{2+}$ which was prepared from the reaction between *trans*-[$CoCl_2$(1,5*R*,7*R*,11-$Me_4$-2,3,2-tet)]$ClO_4$ and (*R*)-alanine.[9] This observation indicates that the above decarboxylation produced predominantly (*R*)-alaninato complex.[10] Actually, the red crystals isolated from the decar-

(1) The fully systematic name is (6*R*,8*R*)-6,8-dimethyl-2,5,9,12-tetraazatridecane.

(2) Asperger, R. G.; Liu, C. F. *Inorg. Chem.* **1967**, *6*, 796–800.

(3) Job, R. C.; Bruice, T. C. *J. Am. Chem. Soc.* **1974**, *96*, 809–819.

(4) Yamaguchi, M.; Yamamatsu, S.; Furusawa, T.; Yano, S.; Saburi, M.; Yoshikawa, S. *Inorg. Chem.* **1980**, *19*, 2010–2016.

(5) Yamaguchi, M.; Yano, S.; Saburi, M.; Yoshikawa, S. *Bull. Chem. Soc. Jpn.* **1980**, *53*, 691–698.

(6) Okawa, H.; Numata, Y.; Mio, A.; Kida, S. *Bull. Chem. Soc. Jpn.* **1980**, *53*, 2248–2251.

(7) Ajioka, M.; Yano, S.; Saburi, M.; Yoshikawa, S. *Inorg. Chem.*, to be published.

(8) Elemental analysis, Anal. Calcd for $C_{15}H_{38}ClCoN_5O_{10.5}$: C, 32.71; H, 6.95; N, 12.71. Found: C, 32.85; H, 6.50; N, 12.25. $^1$H NMR ($D_2O$) 1.08 (d, $J$ = 7.9 Hz, C-$CH_3$), 1.42 (d, $J$ = 6.0 Hz, C-$CH_3$), 1.72 (s, C-$CH_3$ of AMM), 1.92 (s, N-$CH_3$), 2.18 (s, N-$CH_3$) ppm; AB ($H_2O$) $\bar{\nu}_{max}$ 19 300 (log ε = 2.18) 27 000 (log ε = 2.18) cm$^{-1}$; CD ($H_2O$) $\bar{\nu}_{max}$ 18 800 (Δε −0.44) 21 000 (Δε +0.70) 27 500 (Δε −0.36) cm$^{-1}$.

(9) Ajioka, M.; Yano, S.; Toriumi, K.; Ito, T.; Yoshikawa, S., to be submitted for publication. The bromide was converted from the Λ-β$_2$-[Co(*R*-Ala)(1,5*R*,7*R*,11-$Me_4$-2,3,2-tet)]$(ClO_4)_2$·$H_2O$ obtained in the second step of the cycle. The crystals from in the orthorhombic space group $P2_12_12_1$ with $a$ = 11.713 (1), $b$ 20.301(2), $c$ 10.113(2) Å; $Z$ = 4. The structure was solved by heavy-atom methods and refined by full-matrix least-squares procedures with anisotropic temperature factors; $R = \sum||F_o| - |F_c||/\sum|F_o| = 0.054$; $R' = [\sum W(|F_o| - |F_c|)^2/\sum W|F_o|^2] = 0.054$, where $1/W = [\sigma(|F|)]^2 = [\sigma(\text{count})]^2 + [0.015|F_o|]^2$. Tables of the final positional and thermal parameters, bond distances, and bond angles are available as supplementary material.

0002-7863/81/1503-2459$01.25/0 